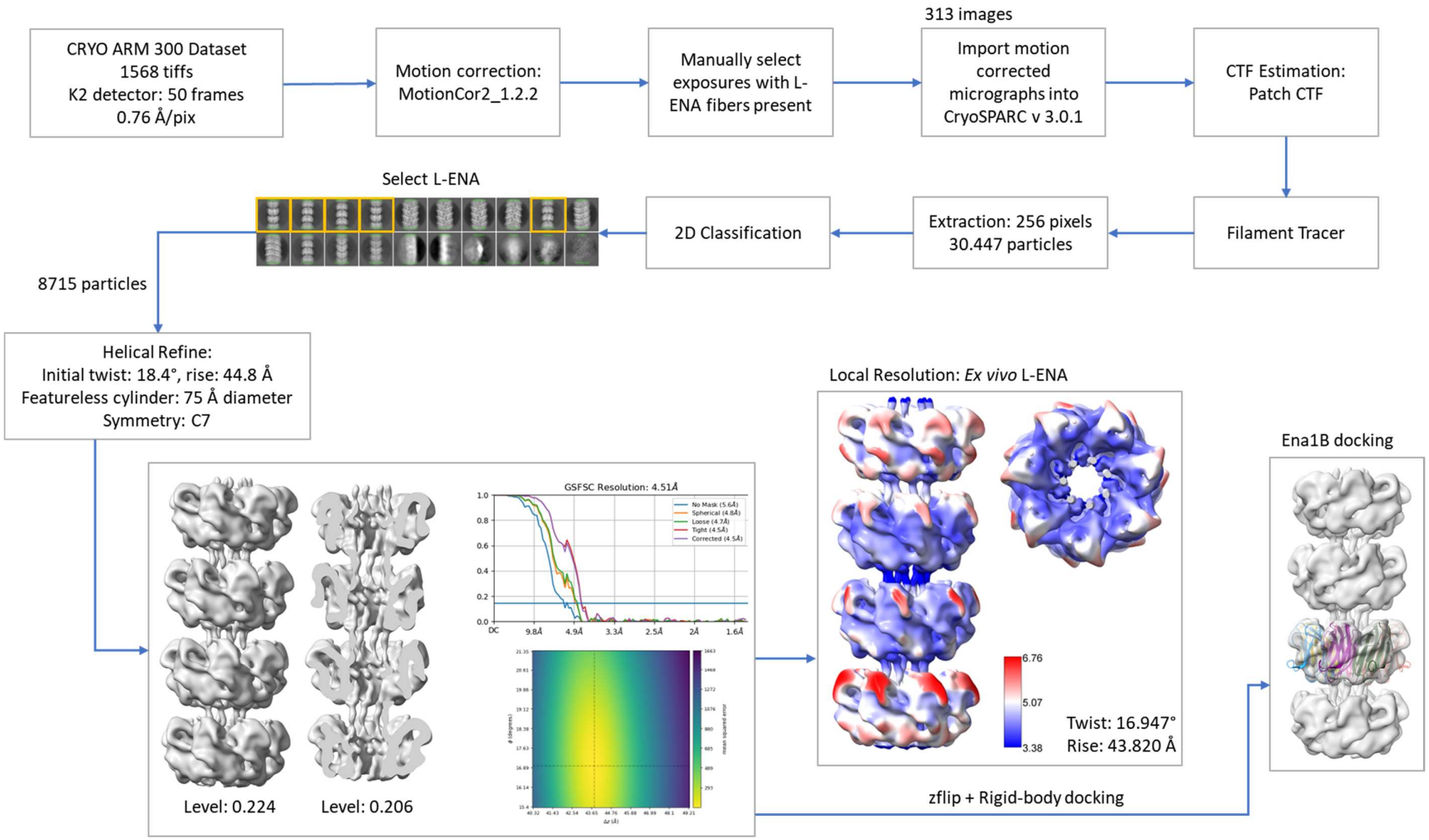

Supplementary Figure 1: CryoEM workflow for the *ex vivo* L-ENA fibers: Cryosparc processing workflow for the *ex vivo* L-type ENA fibers.

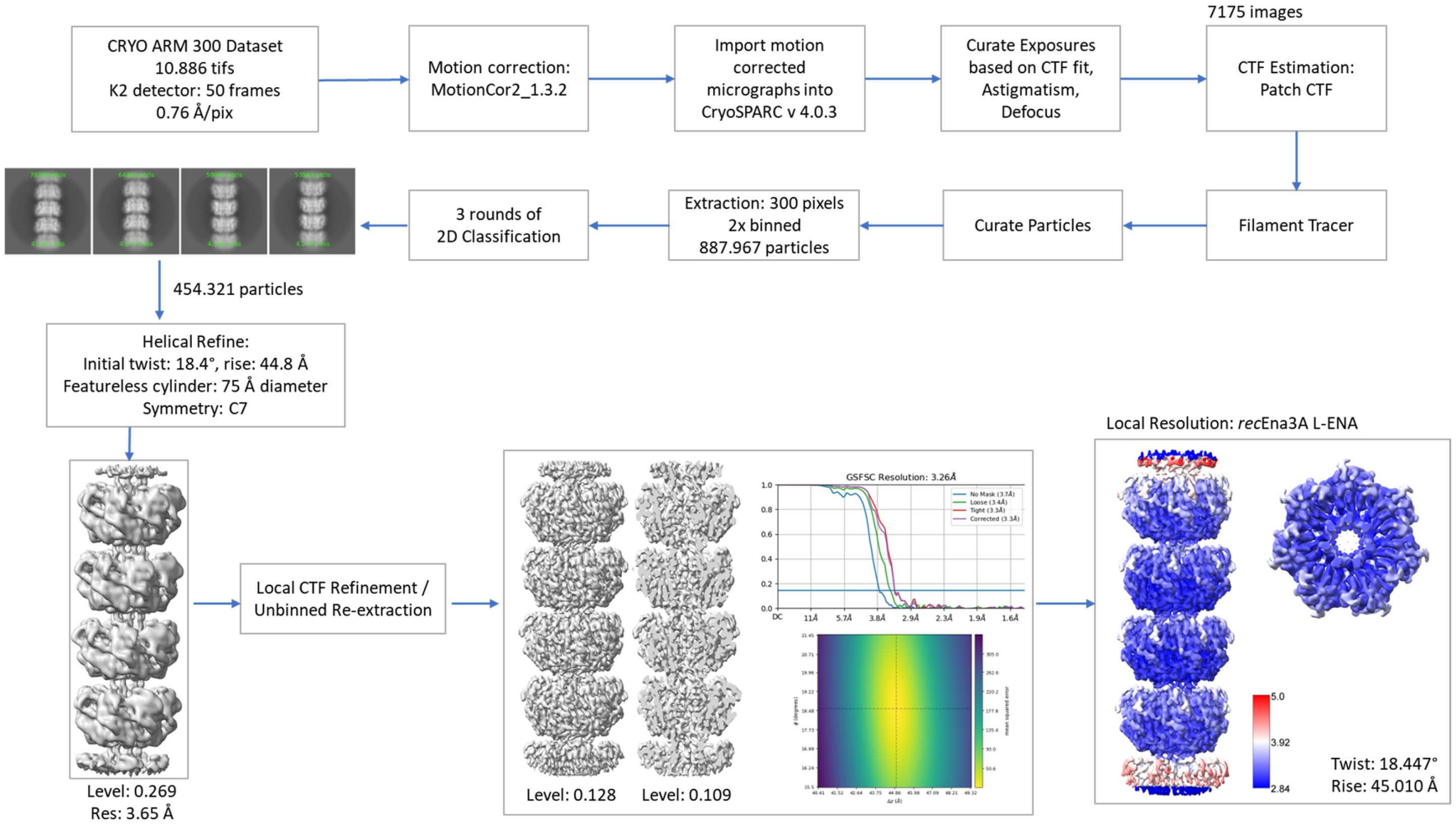

Supplementary Figure 2: CryoEM workflow for the *rec*Ena3A L-ENA fibers: Cryosparc processing workflow for the recombinant L-type ENA fibers.

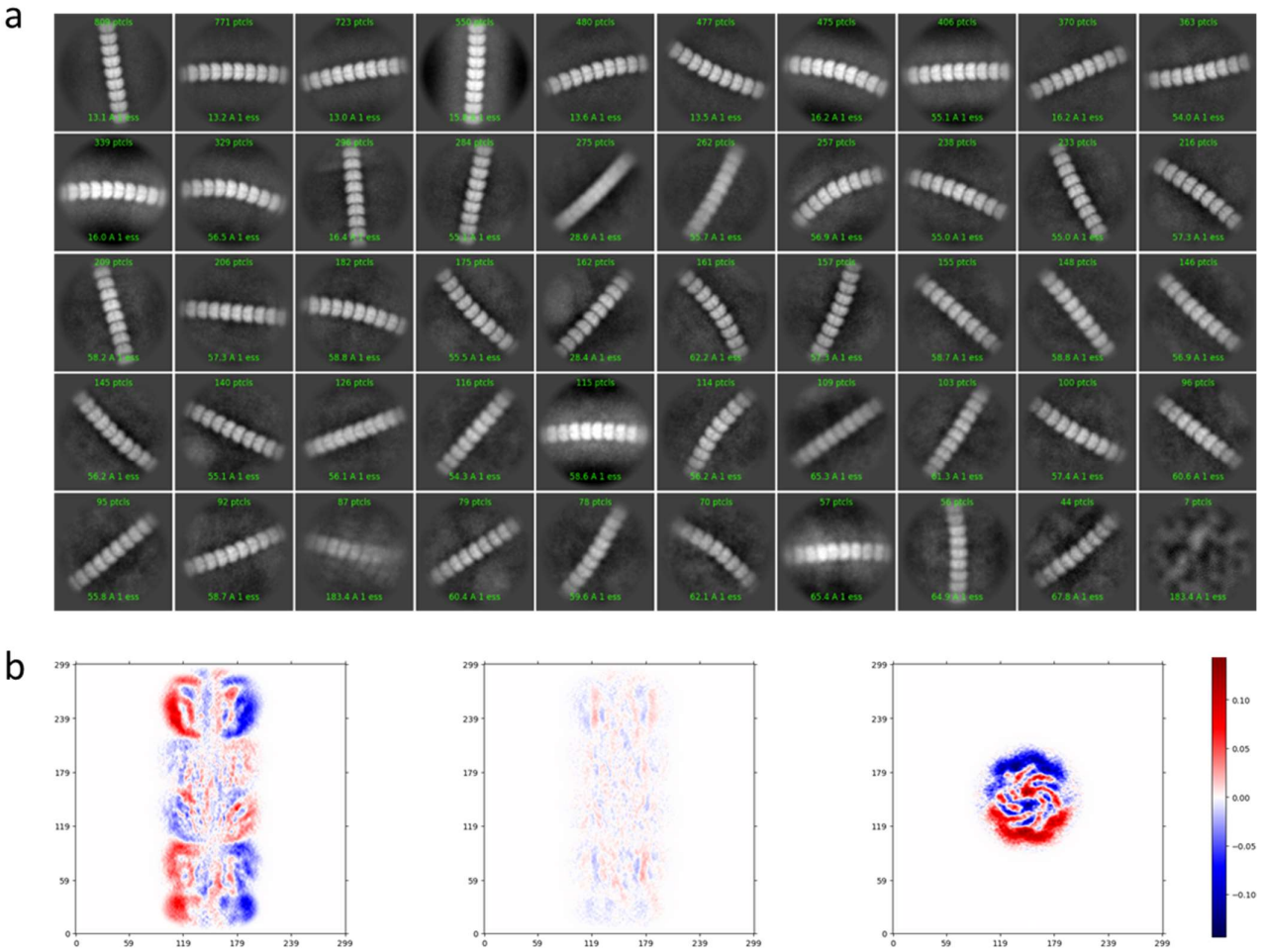

Supplementary Figure 3: Flexibility of *rec*Ena3A L-ENA fibers: (a) CryoSPARC (*1*) 2D class averages of L-ENA using a particle box size of 600x600pixels (0.76Å/pixel) after manual picking of high curvature L-ENA segments, (b) Cryosparc output for the mode 1 of the 3D variability analysis job on L-ENA (see Supplementary Movie 1 for a representation of the corresponding volume series).

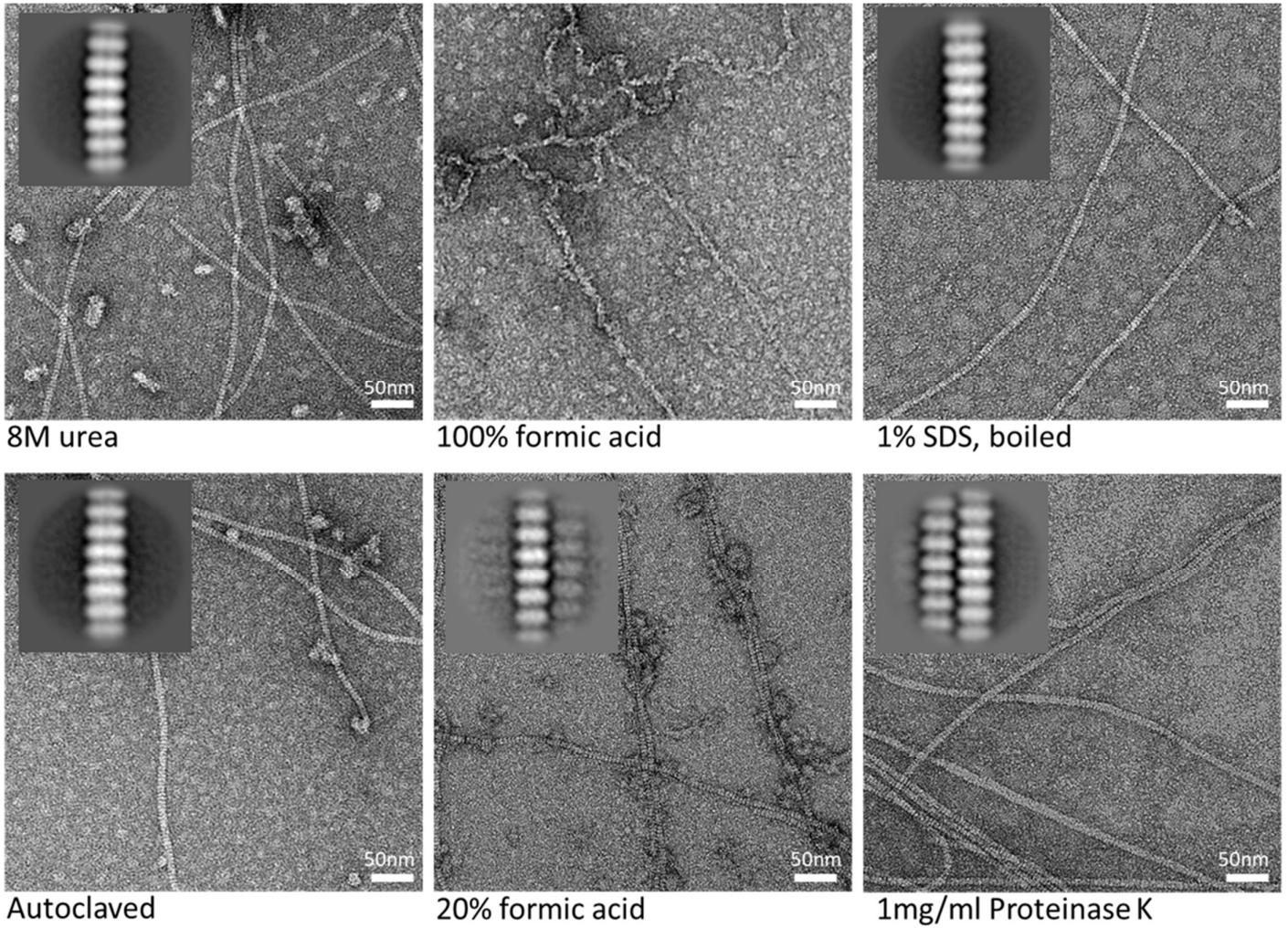

Supplementary Figure 4: Stability assay for recEna3A fibers: recombinant Ena3A fibers were incubated for 1h in 8M urea, 20% or 100% (v/v) formic acid, or boiled in 1% (w/v) SDS, autoclaved (121C° for 18min) in miliQ, or incubated in 1 $mg.mL^{-1}$ proteinase K in 33.3mM Hepes pH 7.5, 1mM $CaCl_2$ for 24h.

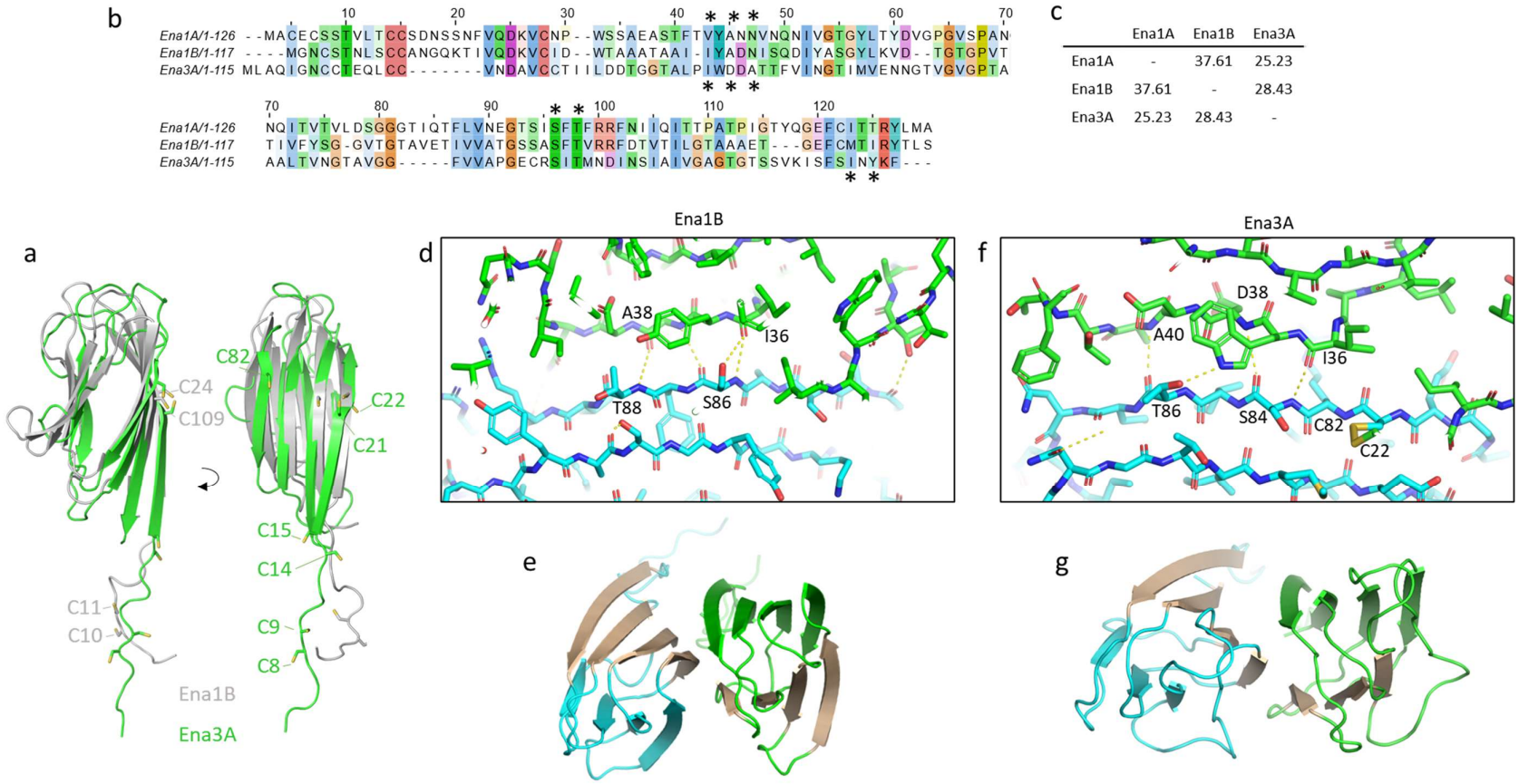

Supplementary Figure 5: Comparison between the major subunits of L- and S-type ENA fibers: (a) Structural comparison between Ena1B and Ena3A, (b) Multiple sequence alignment of the S-ENA subunits (Ena1A and Ena1B) and the L-ENA subunit (Ena3A). Residues involved in lateral contacts are highlighted with a star (above: S-ENA contact; below: L-ENA contacts), (c) percent identity matrix for Ena1A, Ena1B and Ena3A, (d) and (e) comparison between the β-sheet augmentation contacts at the Ena1B dimer interface (PDB: 7A02), and (f) and (g) the β-sheet augmentation at the Ena3A dimer interface. Inter-molecular hydrogen bonds (determined in PyMol 2.5.2 using "Find Polar between Chains") shown in yellow, dashed lines.

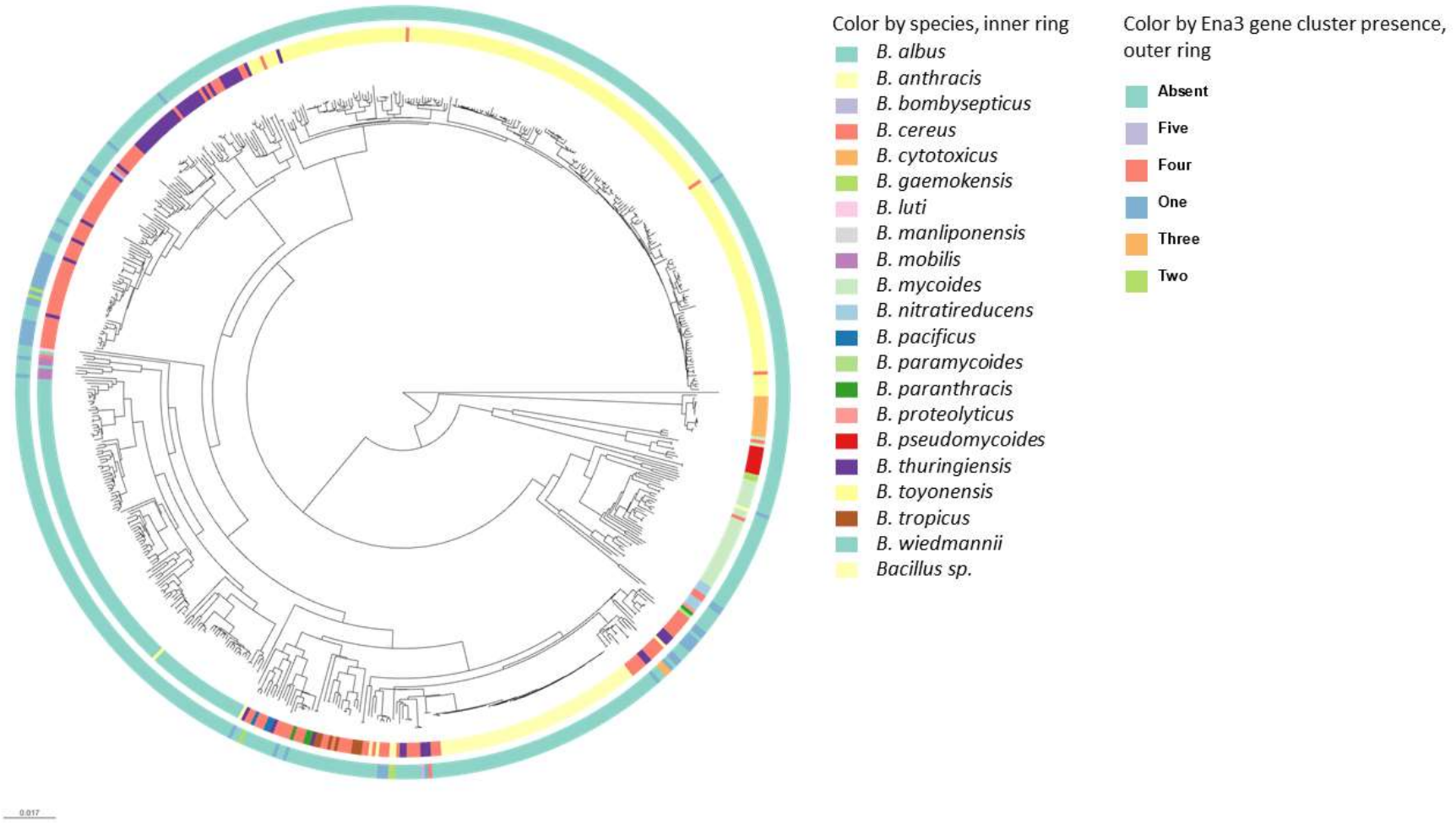

Supplementary Figure 6: Phylogenetic analysis of L-ENA occurrence: Clustering of 656 *B. cereus s.l.* genomes (*B. subtilis* is excluded from tree). Rings are colored according to designated species (inner ring) and presence and copy-number of *ena3A* gene cluster (outer ring). Tree is made using Mashtree (*2*), visualized using Microreact, and available at https://microreact.org/project/uzm4JFrrsCPZeRnMpRqvvf-supplementary-figure-9-ena3-paper.

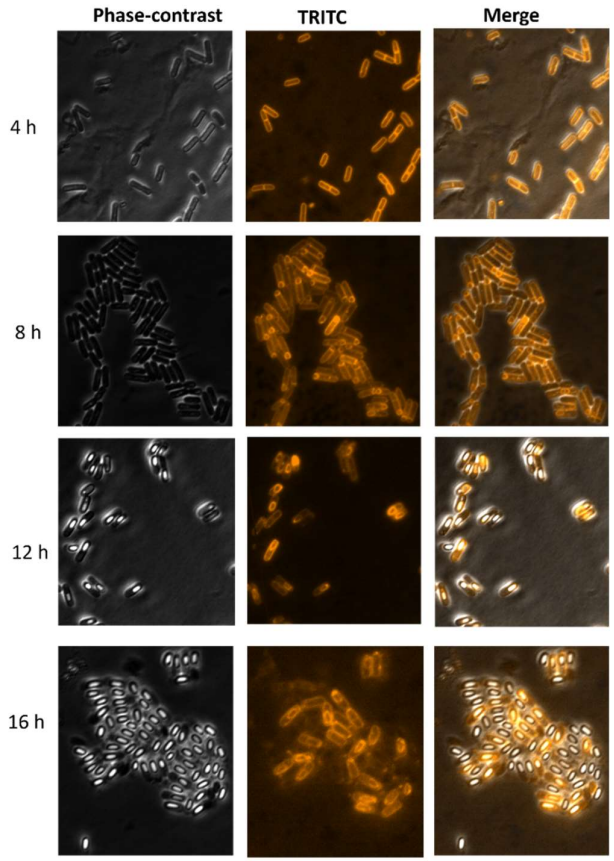

Supplementary Figure 7: Time-course fluorescence microscopy analysis of sporulation in *B. paranthracis* NVH0075-95: At specified time points, cells were stained with 10 µM of FM4-64 dye and examined using a 100x phase-contrast objective of Nikon Eclipse Ti2 fluorescence microscope. Images were processed using Fiji (*3*).

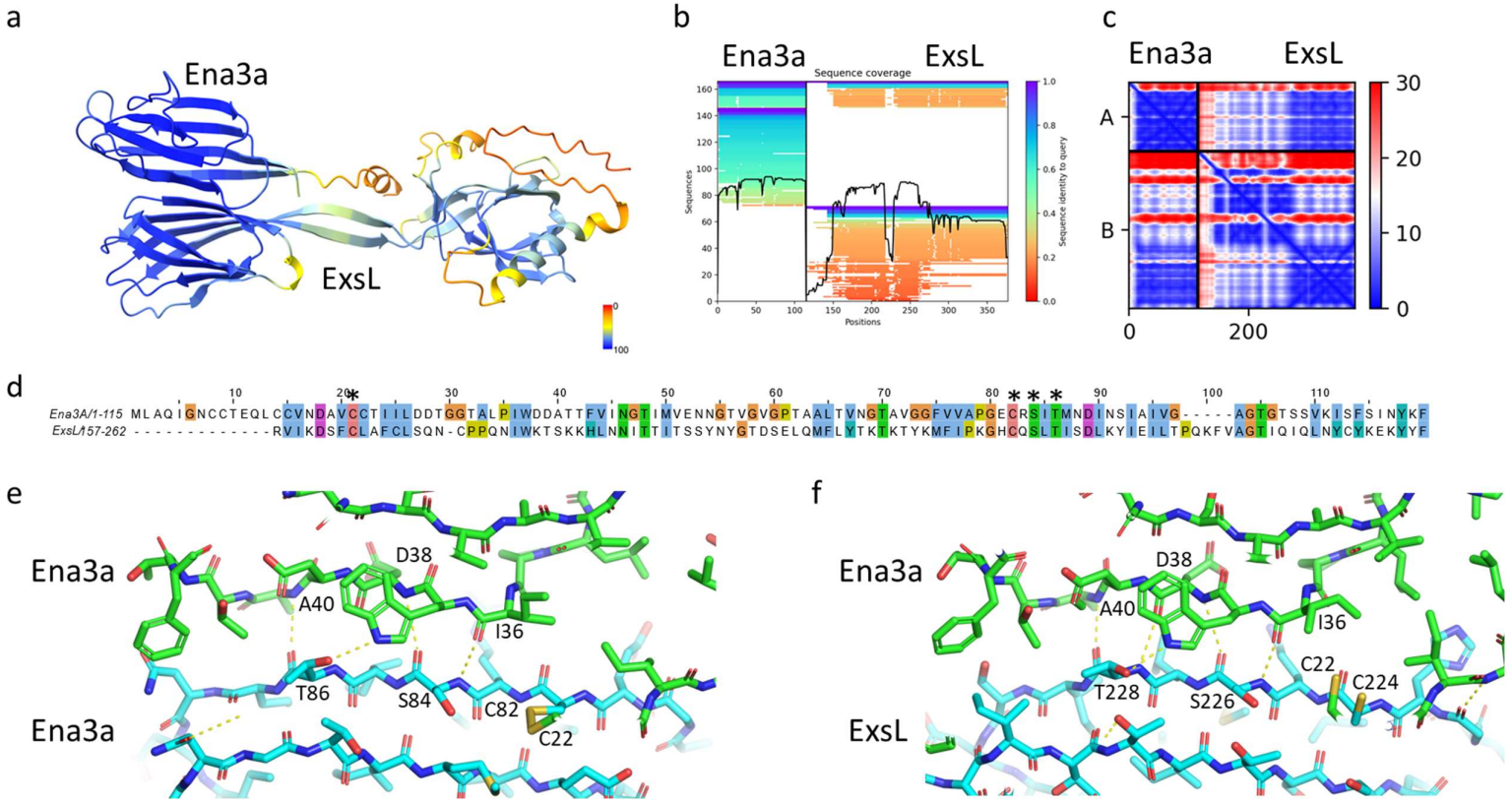

Supplementary Figure 8: Alphafold2 multimer prediction of the ExsL-Ena3A dimeric complex: (a) Alphafold-multimer 1.2 (*4*) ExsL-Ena3A dimer (pLDDT=82.6; ptmscore=0.73) colour coded according to pLDDT-score, (b) Sequence coverage of the corresponding ExsL-Ena3A multiple sequence alignment (source data is provided as a Source Data file), (c) Predicted aligned error map of the predicted ExsL-Ena3A dimer, (d) Pairwise sequence alignment (17.4% sequence identity) of Ena3A and the C-terminal Ena-core domain of ExsL (157-262). Residues involved in lateral Ena3A-Ena3A contacts (highlighted with a star) are conserved in ExsL, (e) β-sheet augmentation at the Ena3A dimer interface (determined via cryoEM), (f) Predicted β-sheet augmentation at the ExsL-Ena3A heterodimer interface (predicted using AF2 multimer). Inter-molecular hydrogen bonds (determined in PyMol 2.5.2 using "Find Polar between Chains") shown in yellow, dashed lines.

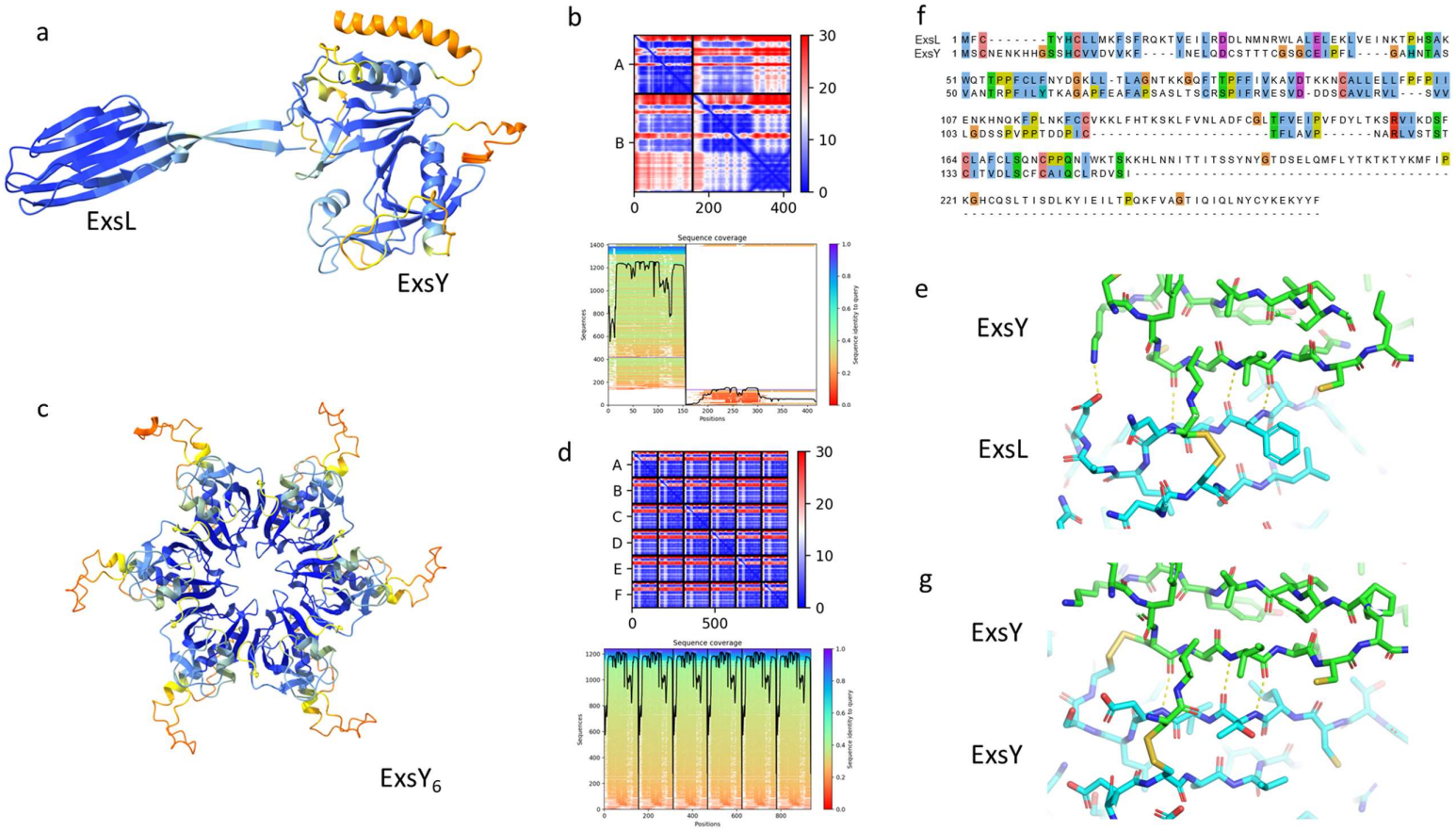

Supplementary Figure 9 : (a) Alphafold-multimer 1.2 ExsL-ExsY dimer (pLDDT=80.2; ptmscore=0.71) colour coded according to pLDDT-score, (b) Predicted aligned error map and sequence coverage (source data is provided as a Source Data file) of the multiple sequence alignment, (c) Alphafold-multimer 1.2 ExsY hexamer (pLDDT=81.3; ptmscore=0.86) colour coded according to pLDDT-score, (d) Predicted aligned error map and sequence coverage (source data is provided as a Source Data file) of the multiple sequence alignment, (e) Pairwise-sequence alignment between ExsL and ExsY (30.8% sequence identity), comparison of the AF2, (f) and (g) comparison of the putative ExsL/ExsY and ExsY/ExsY dimeric interfaces. Inter-molecular hydrogen bonds (determined in PyMol 2.5.2 using “Find Polar between Chains”) shown in yellow, dashed lines.

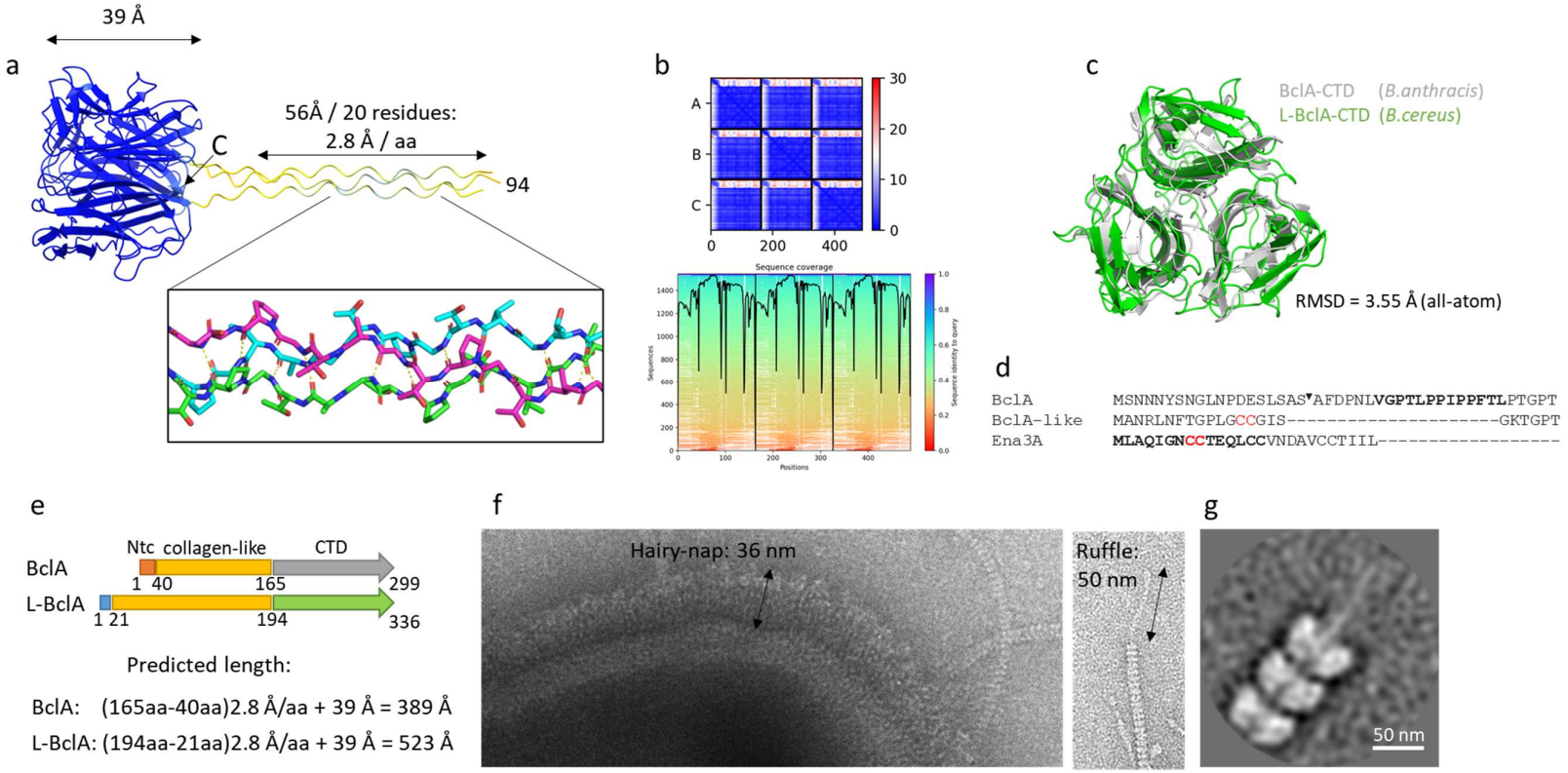

Supplementary Figure 10: Structural analysis of L-BclA: (a) Alphafold-multimer v 1.2 prediction of an L-BclA$_{94\text{-}267}$ trimer (pLDDT=94, ptmscore=0.9) colour coded according to pLDDT-score (N-terminus omitted); collagen-like stalk region shown in stick representation with putative H-bonds shown in dashed lines, (b) Corresponding predicted aligned error map and sequence coverage (source data is provided as a Source Data file) of the multiple sequence alignment of the AF2 L-BclA$_{94\text{-}267}$ trimer, (c) superposition (all-atom RMSD = 3.55Å; sequence identity = 22.1%) of the AF2 L-BclA$_{94\text{-}267}$ trimer with the crystal structure of BclA-CTD of the hairy nap layer of *B. anthracis* (PDB: 1WCK), (d) N-terminal sequence of BclA, L-BclA and Ena3A: letters in bold for BclA correspond to the exosporium leader sequence, and the arrow marker indicates the proteolytic cleavage site. L-BclA has no identifiable exosporium leader sequence, nor any notable sequence homology to the N-terminal connector (shown in bold) of Ena3A apart from a single CC-motif, (e) Domain organization of BclA (Q81JD7) and L-BclA and the corresponding theoretical lengths in fully extended state, (f) Comparison of the thickness of the hairy nap layer to the length of the L-ENA ruffles, (g) 2D class average of L-ENA fiber termini.

Table S1 CryoEM model and data statistics

	Ex vivo L-Ena EMD-17579	*rec*ENA3A EMD-17627; PDB: 8PDZ
Data collection and processing	CryoARM300, BECM	CryoARM300, BECM
Magnification	60.000	60.000
Voltage (kV)	300	300
Electron exposure (e–/Å$_2$)	61.8	63.2
Defocus range (μm)	-0.5 to -3.5	-0.5 to -3.5
Pixel size (Å)	0.766	0.764
Symmetry imposed	Helical Rise = 43.820 Å Twist = 17.041°	Helical Rise = 44.970 Å Twist = 18.547°
Number of segments used	8715	454321
Map resolution (Å) FSC threshold	5.77[1] 0.143	3.32[1] 0.143
Local resolution (Å) (min, 25th percentile, median, 75th percentile, max)	2.63, 4.23, 5.08, 6.66, 11.49	2.84, 3.19, 3.71, 4.96, 8.28
Refinement Initial model used	NA	AlphaFold2
Model resolution (Å) FSC threshold	NA NA	3.3 0.143
Model composition Non-hydrogen atoms Protein residues	 NA NA	 22288 3164
B factor (Å$_2$)	NA	84.18
R.m.s. deviations Bond lengths (Å) Bond angles (°)	 NA NA	 0.004 0.997
Validation MolProbity score Clashscore Poor rotamers (%)	 NA NA NA	 1.47 8.74 0
Ramachandran plot Favored (%) Allowed (%) Disallowed (%)	 NA NA NA	 98.20% 1.80% 0%
Correlation coefficient CC (mask) CC (box) CC (peaks) CC (volume)	 NA NA NA NA	 0.72 0.84 0.70 0.71

1 Numbers reflect the unsharpened map

Table S2. Plasmid constructs

Name	Details	Reference
*p*MAD-I-SceI	Shuttle vector for making deletion mutant, carries I-SceI restriction site	(5)
*p*MAD-I-SceI Δ*ena3A*	pMAD-I-SceI carrying homology sequences flanking *ena3A*	this study
*p*MAD-I-SceI Δ***l-bclA***	pMAD-I-SceI carrying homology sequences flanking *l-bclA*	this study
*p*MAD-I-SceI Δ*exsL*	pMAD-I-SceI carrying homology sequences flanking *exsL*	this study
*p*BKJ233	Expresses I-SceI enzyme (promotes double cross over)	(6)
*p*HT304	Low-copy number plasmid for complementation	(7)
pena3A	pHT304::*ena3A* (complementation of *B. paranthracis* Δ*ena3*A	this study
pl-bclA	pHT304*::l-bclA* (complementation of *B. paranthracis* Δ*l-bclA*)	this study
pexsL	pHT304::*exsL* (complementation of *B. paranthracis* Δ*exsL*)	this study

Table S3. Overview of gene knockout mutants/complementation constructs

Name	**Genetic background**	**Reference**
Wild type	NVH0075-95	(*8*)
Δ*exsL*	NVH0075-95	this study
Δ*l-bclA*	NVH0075-95	this study
Δ*ena3A*	NVH0075-95	this study
Δ*ena1ABC*		(8)
Δ*ena1ABC/***Δ***ena3A*	NVH0075-95 Δ*ena1ABC*	this study
Δ*exsL::pexsL*	NVH0075-95 Δ*exsL*	this study
Δ***l***Δ*bclA::pl-bclA*	NVH0075-95 Δ*l-bclA*	this study
Δ*ena3A::pena3A*	NVH0075-95 Δ*ena3A*	this study
Δ*enaABC/*Δ*ena3A::pena3A*	NVH0075-95 Δ*ena1ABC/*Δ*ena3A*	this study

Table S4. List of primers

Primer code	Sequence (5'-3')	Gene
Quantitative RT-PCR		
2116/2117	AAGTGCGTCTAATCAACAAGGAAA/ GGGAAATCTCCCATGAACACA	*rpoB*
2410/2411	TGGCAAACTACGCCACCTT/ AATTGGCCTTTCTTAGTGTTACCTG	*exsL*
2428/2429	GCAGTAGGTATTGGTGCTGGT/ AAGCGGATACACTTAGAGCTGG	*l-bclA*
2414/2415	CGCAAATAGGAAATTGCTGCAC/ CGGTACCGCCAGTATCATCTAA	*ena3A*
Determining operon		
2311/2312	TGCTGACTTTTGTGGTTTGACT/GGGGCCTGTTTTCCCACTAA	*exsL→l-bclA*
2314/2315	ACAGTGCCTCAATCAGGGAG/CAGCTGTTGGTCCAACTCCA	*l-bclA→ena3A*
Colony PCR screening of mutants and Sanger sequencing		
2241/2242	GGTTGGAGCTGCCTTAACAA/ TGAGGGGTCACCATATCAAAA	*ena3A*
2311/2313	TGCTGACTTTTGTGGTTTGACT/ATCCTCCAACAGCTGTTCCG	*l-bclA*
2363/2364	TTCTTTGGTGGGGATGGGATT/ ACATCCAAGTGGTCCAGTGA	*exsL*
Complementation		**Plasmid**
2374/2375	ACTATGAATTCATGTTTTTATATACTAAAACCAAAACTTATAAAATGTTTATCCCGAA/ GTCAGTGAATTCTTACGAAACCCTAATGATTGTTAAGGCAGC	pHT304-*pl-bclA*

References.

1. A. Punjani, J. L. Rubinstein, D. J. Fleet, M. A. Brubaker, cryoSPARC: algorithms for rapid unsupervised cryo-EM structure determination. *Nat Methods* **14**, 290-296 (2017).
2. L. S. Katz *et al.*, Mashtree: a rapid comparison of whole genome sequence files. *J Open Source Softw* **4**, (2019).
3. J. Schindelin *et al.*, Fiji: an open-source platform for biological-image analysis. *Nat Methods* **9**, 676-682 (2012).
4. E. Richard *et al.*, Protein complex prediction with AlphaFold-Multimer. *bioRxiv*, 2021.2010.2004.463034 (2022).
5. T. Lindbäck *et al.*, CodY, a pleiotropic regulator, influences multicellular behaviour and efficient production of virulence factors in Bacillus cereus. *Environ Microbiol* **14**, 2233-2246 (2012).
6. B. K. Janes, S. Stibitz, Routine Markerless Gene Replacement in Bacillus anthracis. *Infect. Immun.* **74**, 1949-1953 (2006).
7. O. Arantes, D. Lereclus, Construction of cloning vectors for Bacillus thuringiensis. *Gene* **108**, 115-119 (1991).
8. B. Pradhan *et al.*, Endospore Appendages: a novel pilus superfamily from the endospores of pathogenic Bacilli. *EMBO J* **40**, e106887 (2021).